

Deep optical imaging of nova remnants II. A southern-sky sample

C.D. Gill & T.J. O’Brien

Astrophysics Research Institute, Liverpool John Moores University, Byrom Street, Liverpool L3 3AF
e-mail: cdg & tob @astro.livjm.ac.uk

28 August 2021

ABSTRACT

We present an optical imaging study of 20 southern-sky nova remnants which has resulted in the discovery of four previously unknown nova shells – V842 Cen, RR Cha, DY Pup and HS Pup. The study has also revealed previously unobserved features in three other known shells – those of BT Mon, CP Pup and RR Pic. The images of BT Mon, V842 Cen, RR Cha, DY Pup and HS Pup have been processed using several deconvolution algorithms (Richardson-Lucy, maximum entropy and clean) in addition to straightforward point-source subtraction in an attempt to resolve the shells from the central stars. The use of four different methods enables us to make a qualitative judgement of the results. Notably, the shell of RR Pic displays tails extending outwards from clumps in the main ejecta similar to those previously detected in DQ Her.

Key words: novae, cataclysmic variables – circumstellar matter – techniques: image processing

1 INTRODUCTION

In paper I (Slavin, O’Brien & Dunlop 1995) we presented the results of a deep optical imaging survey of the nebular remnants of a sample of northern-sky classical novae. This paper reports on the extension of this survey into the southern-sky using observations made with the Anglo-Australian Telescope in 1995.

Classical nova eruptions result in the ejection of $\sim 10^{-4} M_{\odot}$ of material at velocities of up to several thousand kilometres per second (Bode & Evans 1989). Every nova should be surrounded by an expanding cloud of ejecta and therefore it is perhaps surprising that the literature contains few images of the nova shells themselves. We therefore embarked on an imaging survey of nova remnants taking advantage of the advances in detector technology and image processing techniques that allow us to detect fainter and smaller shells. Since this survey was undertaken we have also been awarded time on the Hubble Space Telescope to image a selected subset of the novae discussed here and in paper I. These data will be presented elsewhere along with the initial results from our kinematical study of the shells.

In the next section we describe the observations and the image processing techniques employed to investigate any extended structure. In section 3 we go on to discuss the observations for each nova for which we detect extended material. Basic data and background information for each of the novae are obtained from Duerbeck (1987) and Bode & Evans (1989). We conclude with a section on estimating distances

via expansion parallax and a brief discussion of the implications of these results.

2 OBSERVATIONS AND IMAGE PROCESSING

The observations were carried out at the Anglo-Australian Observatory on the 3.9-m Anglo-Australian Telescope on 1995 February 23–25. We used TAURUS-2, the Fabry-Perot spectrometer, in direct imaging mode with a Tektronix CCD detector at $f/15$ providing a pixel scale of 0.32 arcsec. All images presented in this paper were taken with an $H\alpha/[N\text{I}]$ filter of central wavelength 6555Å and full width at half maximum 54Å. Table 1 summarizes the observations. Surface brightness estimates of the shells were not attempted as the observing conditions were non-photometric. Also nova shells are known to emit in $H\alpha$ and $[\text{N II}]$, which are both transmitted by the filter used, making measurement of the separate line fluxes impossible. In any case, our primary aim, to detect nova shells and to investigate their morphologies, does not require photometry.

We investigated each image for any initial evidence of extended material using two methods. We compared the nova to two stars taken from the same frame using contour maps of images of each object scaled to the same peak brightness. Figure 1 shows the results for HS Pup, an object for which we claim to have detected extended emission, and GI Mon, for which there was no evidence of extension. We

arXiv:astro-ph/9806076v1 4 Jun 1998

Nova	Integration	t_3 time	Seeing	Extended?	Shell Size
	time / s	/ days	FWHM / arcsec	(Yes/No)	/ arcsec
V365 Car	900	530	1.7	N	
MT Cen	1800	–	1.0	N	
V359 Cen	2×900	–	1.6	N	
V842 Cen	4×400+200	48	0.7	Y	< 1.5
RR Cha	1800	60	0.8	Y	3×2
AR Cir	1800	415	0.6	N	
AP Cru	2×900	–	2.0	N	
BT Mon	2×900	36 / 190 ¹	1.8	Y	11×9
GI Mon	2×900	23	1.0	N	
GQ Mus	2×900	45	1.8	N	
IL Nor	1800	108	0.6	N	
V841 Oph	2×900	130	0.7	N	
V972 Oph	1800	176	2.0	N	
RR Pic	1800	150	1.1	Y	30×21
CP Pup	1800	8	1.2	Y	19.5
DY Pup	1800	160	0.8	Y	7×5
HS Pup	1800	65	0.8	Y	< 2.5
HZ Pup	2×900	70	1.7	N	
XX Tau	2×900	42	1.6	N	
CQ Vel	1800	50	1.1	N	

Table 1. The novae imaged at H α /[NII] are listed together with the integration times (the components of co-added images are listed if appropriate), their speed class in terms of t_3 (the time in days taken to decline by three magnitudes from peak brightness), the seeing measured from each image in arcsec, whether the nova appeared to be extended beyond a normal point-spread function and if so, its approximate diameter. Note 1 – the t_3 time for BT Mon is disputed in the literature (see text).

also present, in Figure 2, azimuthally averaged brightness profiles for each of the novae described in section 4 for which we believe we have detected extended emission. In each case the nova light profile is compared with several stars taken from the same frame. The only difficulty with these methods is when the star and the nova are of significantly different peak brightness, in which case one or the other will fade into the sky whilst the other is still detectable. In order to avoid confusion due to this effect we have presented our results for each method only up to a radius where the star or nova brightness is more than 1 sigma above the mean sky level.

If the methods described above led us to believe that extended emission might be present then several techniques were used to try to determine the morphology of this material in more detail.

The most basic of these was straight-forward star subtraction. We selected a star from the same frame as each nova (a brighter star was used to ensure adequate signal to noise in the wings of the point-spread function), this was shifted to the same centroid as the nova, scaled to the same peak intensity and subtracted from the nova image.

We also attempted to deconvolve the nova images using maximum entropy (MEM) and Richardson-Lucy (LUCY) routines available in the UK Starlink Software Collection. The final processing technique used was our own CLEAN routine (for further details see Slavin, O'Brien & Dunlop 1994). The use of a variety of processing techniques enables us to judge, at least qualitatively, whether structure in the extended material is real or simply an artefact of a particular algorithm. As can be seen in the next section, the results from these techniques proved to be in broad agreement.

3 IMAGES OF THE NOVA SHELLS

3.1 V842 Centauri

V842 Cen (Nova Cen 1986) was discovered on 1986 November 22. Maximum light was missed but the t_3 time (the time taken to decline three magnitudes from peak brightness) was estimated to be 48 days by Sekiguchi et al. (1989) and it is therefore classified as a moderately fast nova.

To prevent saturation of the very bright central star, V842 Cen was observed for 4 separate integrations of 400s and 1 integration of 200s. These were then co-added to form the final image shown in Figure 3(a). By comparison with a star from the same frame of slightly higher peak brightness it is clear that V842 Cen is extended beyond a normal PSF, e.g. Fig. 2(b).

The results from the four image processing techniques are displayed in Figure 3(b-e). The star-subtracted image (Fig. 3b) shows a bright ring with radius of approximately 0.8 arcsec. The peak brightness of this ring is about 38% of the peak brightness of V842 Cen's central star and when a field star and the nova are both scaled to the same peak brightness we find that the nova has a total luminosity of twice that of the star. This is clear evidence for bright, somewhat extended, emission-line material.

The LUCY deconvolution is shown in Fig. 3(c) whilst the result of the MEM deconvolution is displayed in Fig. 3(d). The LUCY deconvolution produces a bright small ring comparable with the pixel scale whereas the MEM deconvolution fails to resolve the ejecta from the central source, producing a wide smooth single PSF. The CLEAN technique, Fig. 3(e), does deconvolve the nova into a central point source and a ring. This latter technique employs 2× super-pixellation (linearly interpolating the image onto a grid with half the original pixel scale) prior to deconvolution and the results

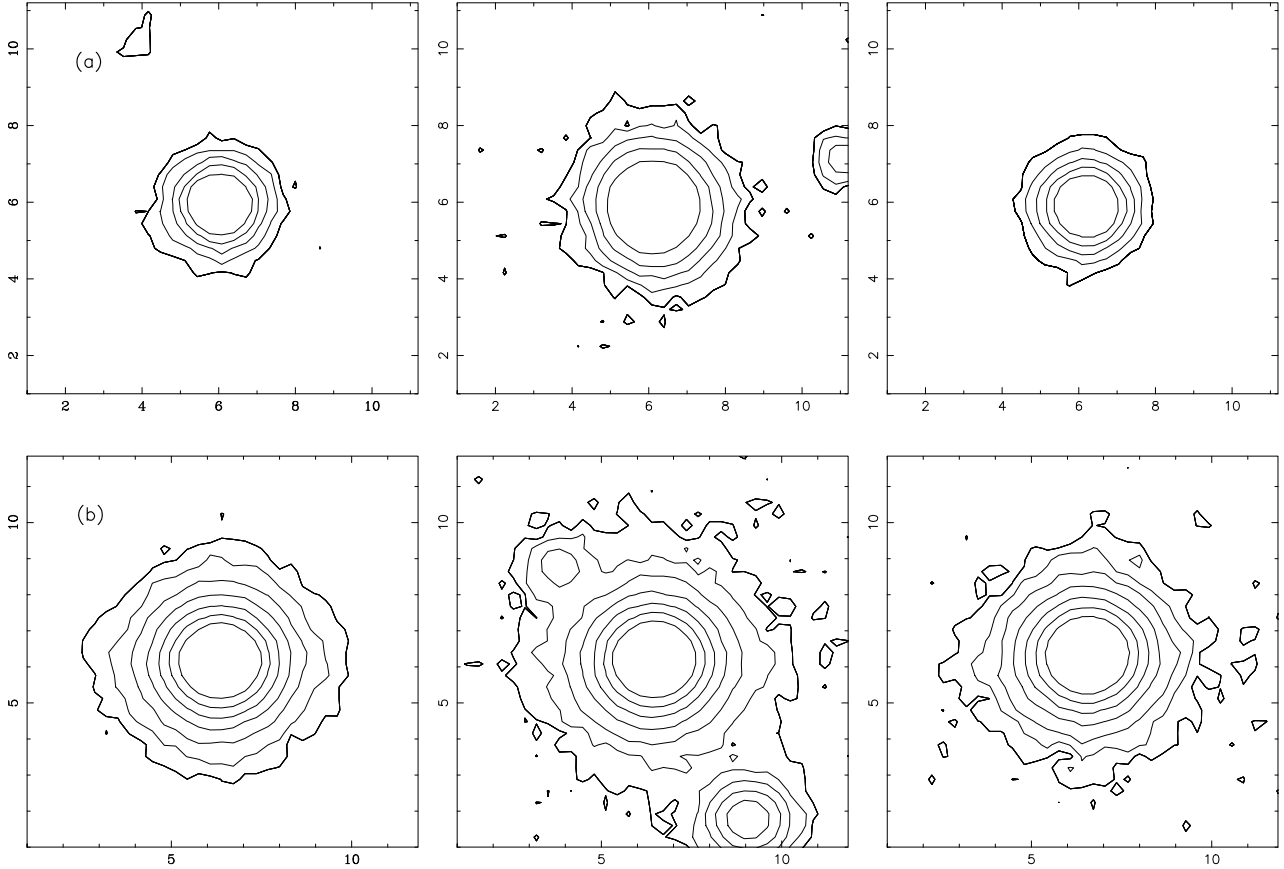


Figure 1. Top panel (a): Contour map of HS Pup (centre) and two scaled down brighter stars from the same frame (on either side) displayed at contours of 0.128, 0.064, 0.032, 0.016 and 0.008 of the peak flux. Lower panel (b): Contour map of GI Mon (centre) and two scaled down brighter stars from the same frame (on either side) displayed at contours of 0.128, 0.064, 0.032, 0.016, 0.008, 0.004 and 0.002 of the peak flux. The final contour in both sets of images is two sigma above the sky background. Axes are marked in arcsec.

are smoothed with a 0.64 arcsec FWHM Gaussian. The CLEAN procedure is bound to result in a central point source as this simply represents the position of peak brightness in the original image. We believe that the MEM method failed to resolve the shell because the shell is so small in comparison to the seeing and the pixel scale. However if this method is used on the super-pixelated data then it results in a ring but no central star (Fig. 3f) comparable to the result from the LUCY deconvolution. The non-detection of a central source is presumably because the shell is so bright and a ring of emission is the simplest model consistent with the data. Clearly these results have to be treated with some caution but as the shell is so bright, it is a good candidate for observations with the Hubble Space Telescope or from the ground in years to come as it increases in size and becomes easier to resolve from the central star.

3.2 RR Chamaeleontis

Maximum light was also missed for RR Cha. It occurred between April 8 and July 13 in 1953. However, the t_3 time has been estimated to be 60 days.

RR Cha was imaged for one integration of 1800s, Fig 4(a). This was possible due to the relative faintness of the central star. The star subtracted frame is shown in Fig. 4(b). The results have been smoothed using a 1.28 arcsec Gaus-

sian to allow faint residual emission to be seen clearly above the noise. The extended material takes the form of an elliptical ring with a major axis of 3 arcsec and minor axis 2 arcsec. The brightest parts of the ring are on the major axis.

The result of the LUCY deconvolution of RR Cha is shown in Fig. 4(c). This looks very similar to the star-subtracted image. The MEM deconvolution is shown in Fig. 4(d). In this case the extended material takes the form of blobs rather than a complete ring but these are located at the same positions as the brightest parts of the ring seen in (b) and (c). A similar result is found from the CLEAN routine, Fig. 4(e).

3.3 BT Monocerotis

BT Mon reached maximum in September 1939. The t_3 time is disputed in the literature due to the exact date of maximum light being missed. Payne-Gaposchkin (1957) quotes a t_3 of 36 days calculated from spectral data whereas Schaefer & Patterson (1983) quote a t_3 of 190 days from the light curve after maximum. This relies on the nova having a plateau of 8.5 magnitudes at maximum whereas Payne-Gaposchkin argues that the spectra imply that BT Mon could have been as bright as mag. 5.0. To complicate mat-

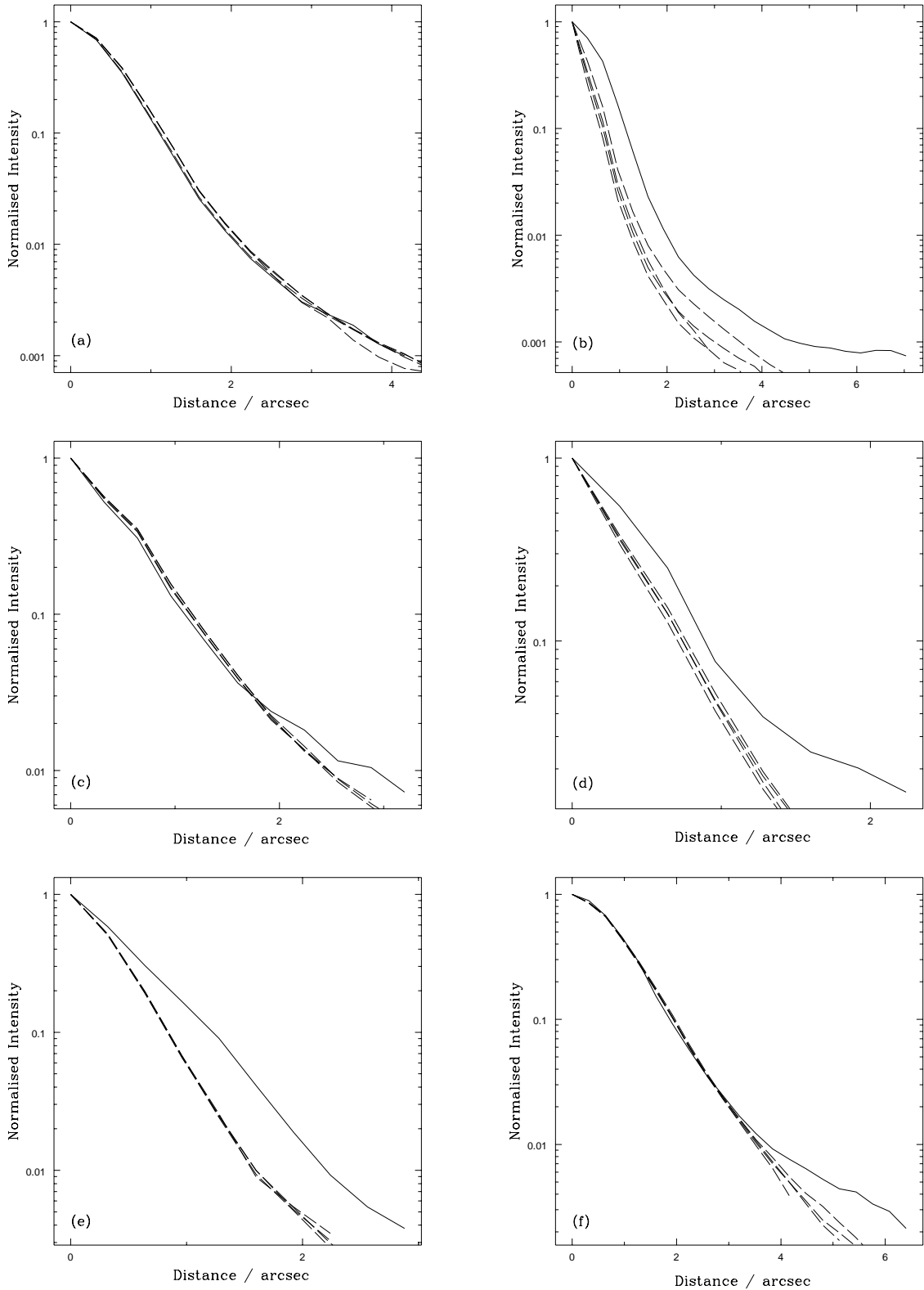


Figure 2. Azimuthally-averaged brightness profiles for several images from our survey. In each case solid lines designate the nova and dashed lines denote 4 field stars taken from the same frame. All profiles are shown down to a cut off one sigma above the sky. a) GI Mon – no obvious extended material (shown for comparison). b) V842 Cen – clearly extended over the whole radial range. c) RR Cha – the nova follows a stellar profile out to about 2 arcsec where some extended material becomes apparent. d) DY Pup – apparently slightly extended over the whole range but with a large increase at about 2 arcsec. e) HS Pup – clearly extended at all distances shown. f) BT Mon – no obvious extended material until a radius of about 4 arcsec.

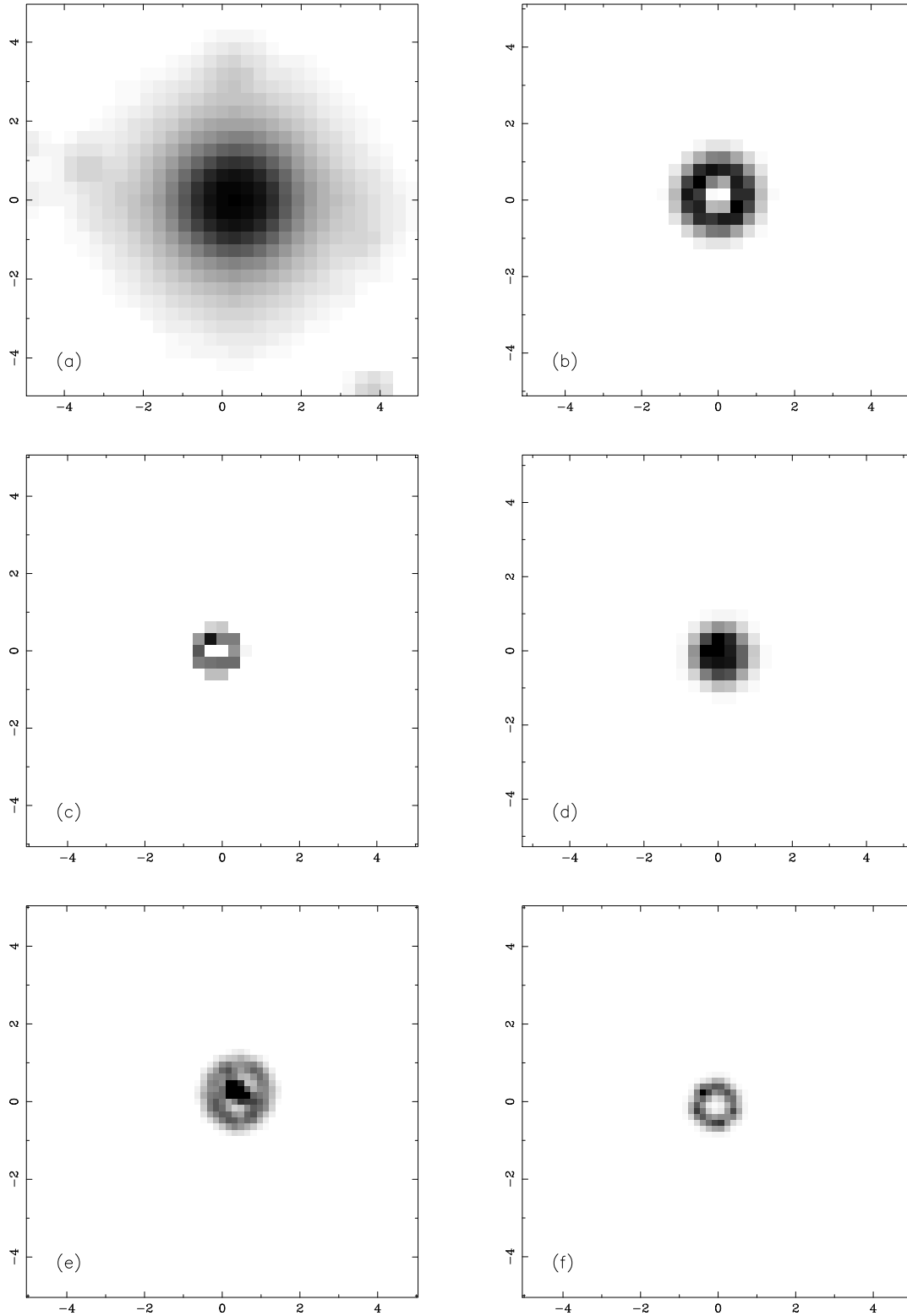


Figure 3. $H\alpha/[NII]$ images of the remnant of V842 Cen. In all five plots north is up, east is to the left and the axes are marked in arcseconds. The images are: a) the original frame shown as a logarithmically grey scaled image, b) the star-subtracted image of the remnant, c) LUCY deconvolved image of the remnant, d) MEM deconvolved image of the remnant, e) CLEANed image of the remnant, and f) super-pixellated MEM deconvolved image of the remnant.

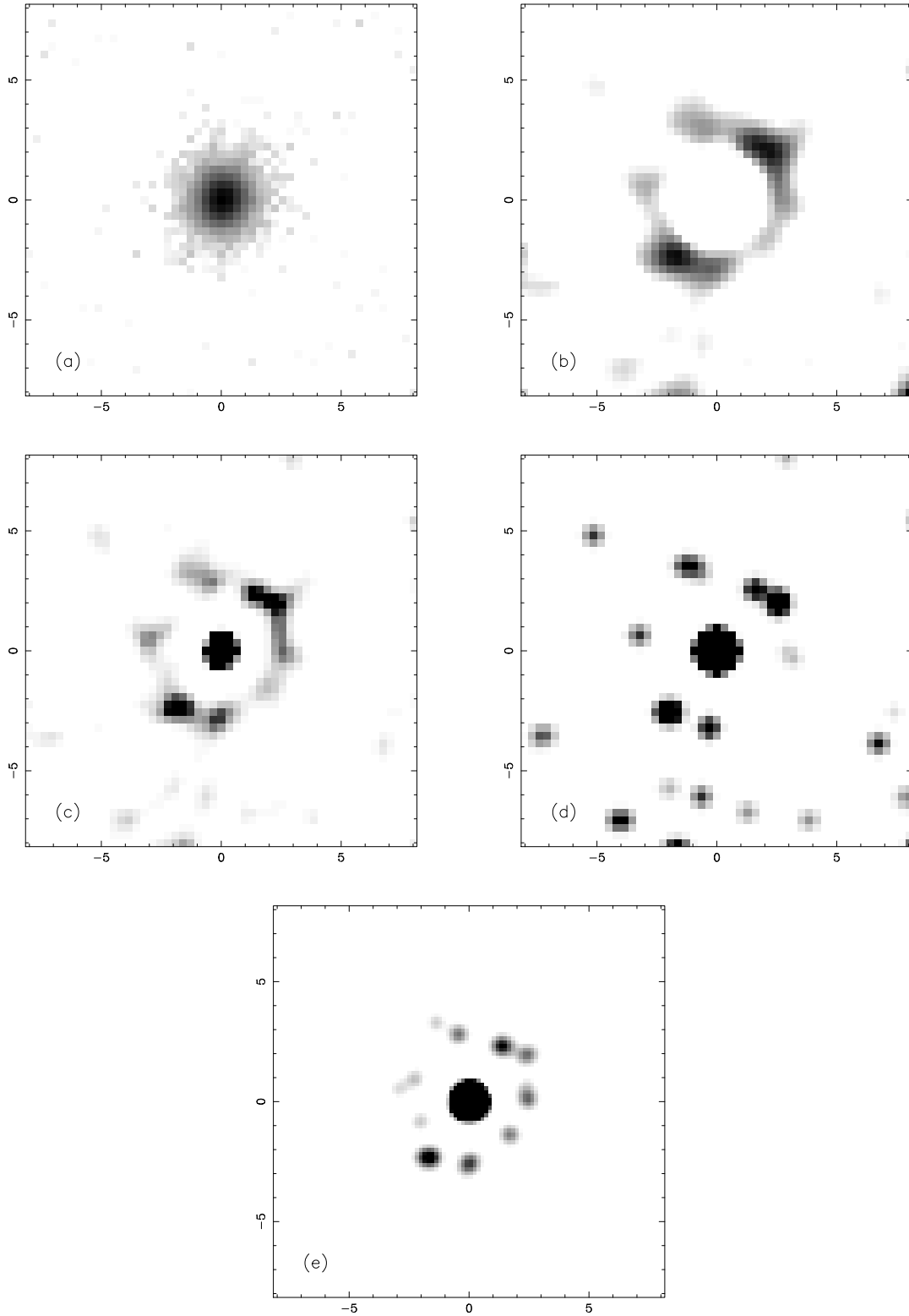


Figure 4. $H\alpha/[NII]$ images of the remnant of RR Cha. In all five plots north is up, east is to the left and the axes are marked in arcseconds. The images are: a) the original frame shown as a logarithmically grey scaled image, b) star subtracted image of the remnant (smoothed with a 1.28 arcsec FWHM Gaussian), c) LUCY deconvolved image of the remnant, d) MEM deconvolved image of the remnant, and e) CLEANED image of the RR Cha remnant (smoothed with a 0.64 arcsec FWHM Gaussian).

ters Duerbeck (1987) describes BT Mon as a ‘probably fast nova’ quoting from Duerbeck (1981) a t_3 of 42 days.

BT Mon has been found to be an eclipsing system with a period of $8^h 1^m$ and therefore we are looking at the system approximately edge-on. The shell has been detected around this nova in spectroscopic observations by Marsh et al. (1983). They determine a distance of 1800 pc to BT Mon assuming the shell, with a diameter of 7 arcsec, was expanding at 1500 km s^{-1} . The slit position used was running east–west over the central star. No direct images of the nebula have been reported that show any clear morphological structure.

Fig. 5(a) shows the image of BT Mon resulting from co-adding two 900s exposures. If one takes into account that the field star to the north is about 30% brighter than BT Mon itself then it is possible to see that the wings of the BT Mon point spread function do extend out further than those of this nearby star, indicating the presence of some nebular material.

The results of star subtraction are displayed in Fig. 5(b). Both stars have been subtracted and the result has then been smoothed using a 0.64 arcsec FWHM Gaussian (2 pixels). The LUCY result is shown in Fig. 5(c), the MEM result in (d) and the CLEANED image in (e). All processes show an incomplete clumpy, slightly elliptical ring with approximate dimensions of 11×9 arcsec and a major axis extending in the north–west–south–east direction. The brightest material running east–west discovered by Marsh et al. (1983) in 1981 was found to have a diameter of 7 arcsec. As BT Mon underwent eruption in 1939 then if we assume this material is moving at a constant velocity then it should have a diameter of 9.3 arcsec in 1995, when these observations were taken. The values measured from our deconvolved images are about 10 arcsec which is in broad agreement with the predicted value.

3.4 RR Pictoris

RR Pic is a well-studied old nova. It reached maximum in 1925 with an apparent visual magnitude of 1.0. It had a t_3 of 150 days which characterises it as a slow nova. The period of the central system has been measured at $3^h 28^m 50^s$

The extended shell has been known for a long time. The first material to be detected was by van den Bos and Finsen in the early 1930’s (see Williams & Gallagher (1979) and references therein) who observed bright knots on opposite sides of the central system which they observed to be moving away from the centre over 3 years with position angles (PAs) of 70° and 230° and a separation of 2 arcsec in 1931. Apparently the next observations of the shell were made by Williams & Gallagher (1979) who again detected these knots. By this time they had a total separation of 23 arcsec implying a constant rate of expansion since 1931. The latest published image of RR Pic found in the literature was in Evans et al. (1992) (hereafter E92). The image therein resembles our own, shown in Fig. 6(b), apart from the fact that our image appears to have much better spatial resolution.

The deconvolution techniques could not be safely used on the image of RR Pic as there were no unsaturated stars in the frame brighter than the nova central system itself. If a fainter star were used to characterise the PSF then its

wings would disappear into the noise before those of the central system of RR Pic leading to spurious detection of extended material. However, the shell is so large and clearly detected in our images that deconvolution is not necessary.

The image of RR Pic is shown at two levels in Fig. 6. Fig. 6(a) has been displayed with scaling chosen so that the brighter equatorial ring can be seen. This feature has a major axis of 21 arcsec at a position angle of approximately 150° . Fig. 6(b) has been displayed so that the fainter material and tails running out to the north–east and south–west can be seen. O’Brien & Slavin (1996) investigated the tails using the same image processing technique employed by Slavin, O’Brien & Dunlop (1995). An image taken through a $[\text{NII}]6594\text{\AA}$ filter shows only the southwest half of the equatorial ring indicating that this side of the shell is tilted away from the observer (whether the emission is intrinsically $\text{H}\alpha$ or $[\text{NII}]$).

Assuming a constant rate of expansion for the knots shown in Williams & Gallagher (1979) then we expect them to have a total separation in 1995, when these images were taken, of 30 arcsec. The separation of the knots on our image is indeed 30 arcsec.

3.5 CP Puppis

CP Pup reached maximum light on 1942 November 9 and faded very quickly with a t_3 time of 8 days classifying it as a very fast nova. The shell was first resolved by Zwicky (see Bowen 1956) and the latest image found in a search through the literature was in Williams (1982). He shows an $\text{H}\alpha + [\text{NII}]6584\text{\AA}$ image taken at the CTIO 4m telescope in 1980 with an exposure of 4500 seconds onto a baked 098-04 plate which only just detects the clumpy shell of diameter 14 arcsec.

There has been no attempt to deconvolve the image of CP Pup, shown in Fig. 7, for the same reasons as RR Pic. In Williams (1982) the peak to peak diameter of the shell in the NW to SE and NE to SW directions is approximately 10 arcsec. If we assume constant expansion since that image was taken in 1980 then the shell size in our observation should be about 14 arcsec. The measured peak to peak diameters in these directions are 15 and 14.5 arcsec respectively which is in broad agreement with constant expansion.

3.6 DY Puppis

DY Pup reached maximum in November 1902 and declined slowly with a t_3 of 160 days. Little other work has been done on this nova with no spectroscopic information available.

The raw image of DY Pup and its surroundings resulting from a single 1800s integration is shown in Fig. 8(a). It is possible to make out some very faint extended material although the object just to the north–east of DY Pup appears to be a field star.

The star subtracted image is shown in Fig. 8(b). In this case, both the central star and the nearby field star have been subtracted and the residual smoothed using a 2 arcsec FWHM Gaussian. The result is a ring of material with enhancements to the north–east, north–west, south–east and south–west. It appears to be slightly elongated in the north–west–south–east direction. The LUCY deconvolved image is

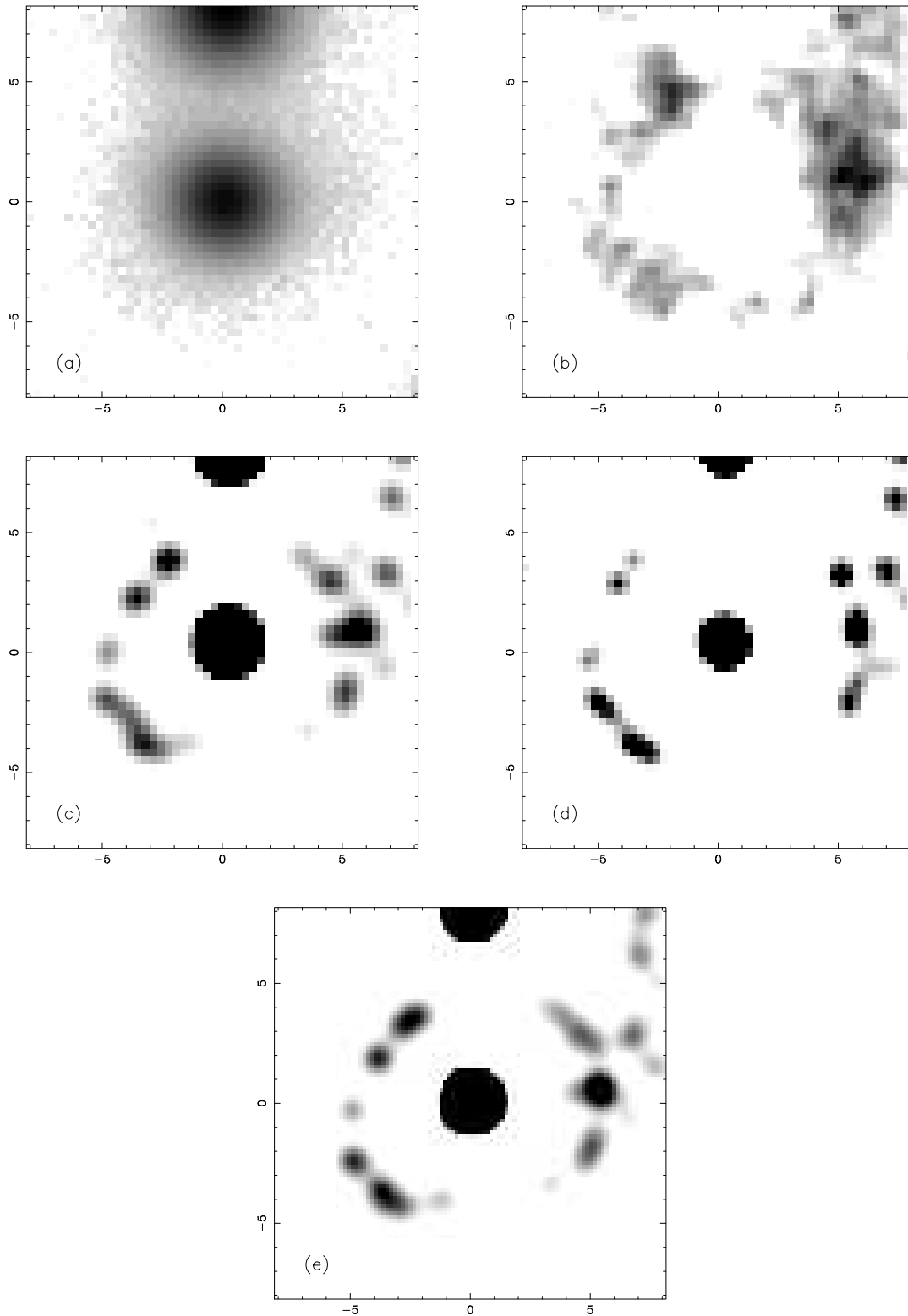


Figure 5. $H\alpha/[NII]$ images of the remnant of BT Mon. In all five plots north is up, east is to the left and the axes are marked in arcseconds. The images are: a) the original frame shown as a logarithmically grey scaled image, b) star subtracted image of the remnant (smoothed using a 0.64 arcsec Gaussian), c) LUCY deconvolved image, d) MEM deconvolved image, and e) CLEANED image (smoothed with a 0.64 arcsec FWHM Gaussian).

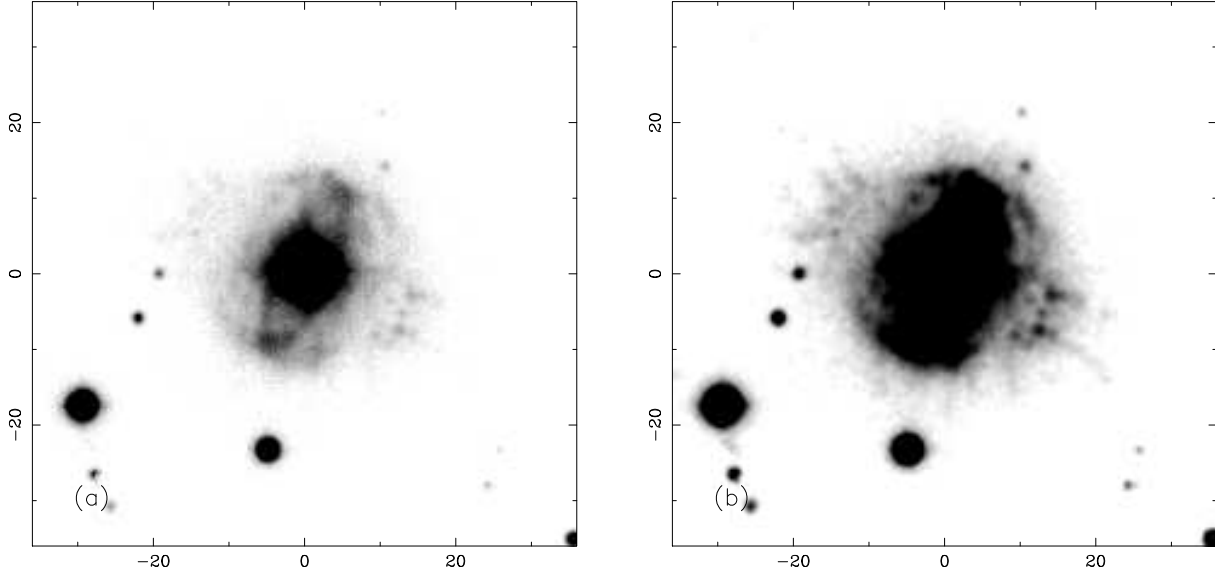


Figure 6. $H\alpha/[NII]$ images of the remnant of RR Pic. North is up, east is to the left and the axes are marked in arcseconds. The same image is displayed at different levels in order to emphasise different features. In a) the bright equatorial ring is apparent whilst in b) the fainter emission and tails orthogonal to the major axis of the ring are more clearly seen.

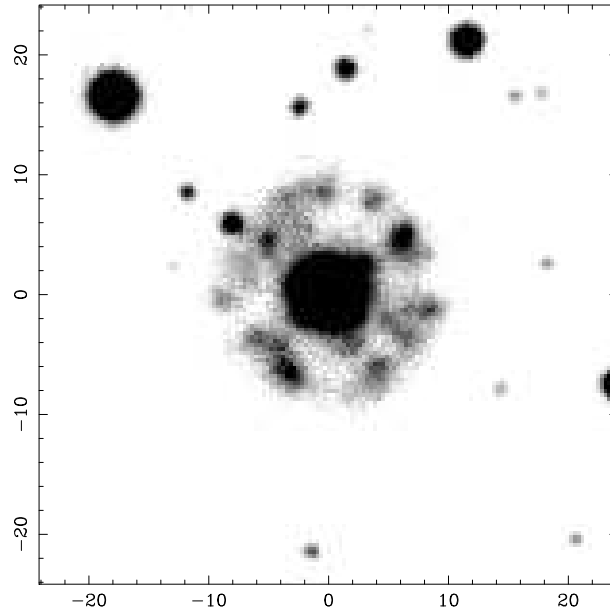


Figure 7. $H\alpha/[NII]$ image of the remnant of CP Pup. North is up, east is to the left and the axes are marked in arcseconds.

shown in Fig. 8(c). The two stars are picked out clearly leaving an extended ring around DY Pup bearing a close resemblance to the results of star subtraction. The MEM result for DY Pup, Fig. 8(d), reveals the same morphology as does the CLEAN result, shown in Fig. 8(e).

3.7 HS Puppis

HS Pup underwent outburst in late December 1963. It reached maximum light on the 23rd at an apparent photographic magnitude of 8.0. It decreased in brightness at a

moderately fast rate with a t_3 of 65 days. There is little data on the nova since then other than its light curve.

The original image resulting from a single 1800s exposure is shown in Fig. 9(a). There is no obvious extended material but, like V842 Cen, when compared with a star scaled to the same peak value, its brightness profile extends out a lot further from the centre of the star (Fig. 2e).

The star subtracted image is displayed in Fig. 9(b). The LUCY deconvolution is shown in Fig. 9(c). It has resolved the object into a central star and a surrounding halo of radius approximately 1 arcsec. The MEM deconvolution, Fig. 9(d),

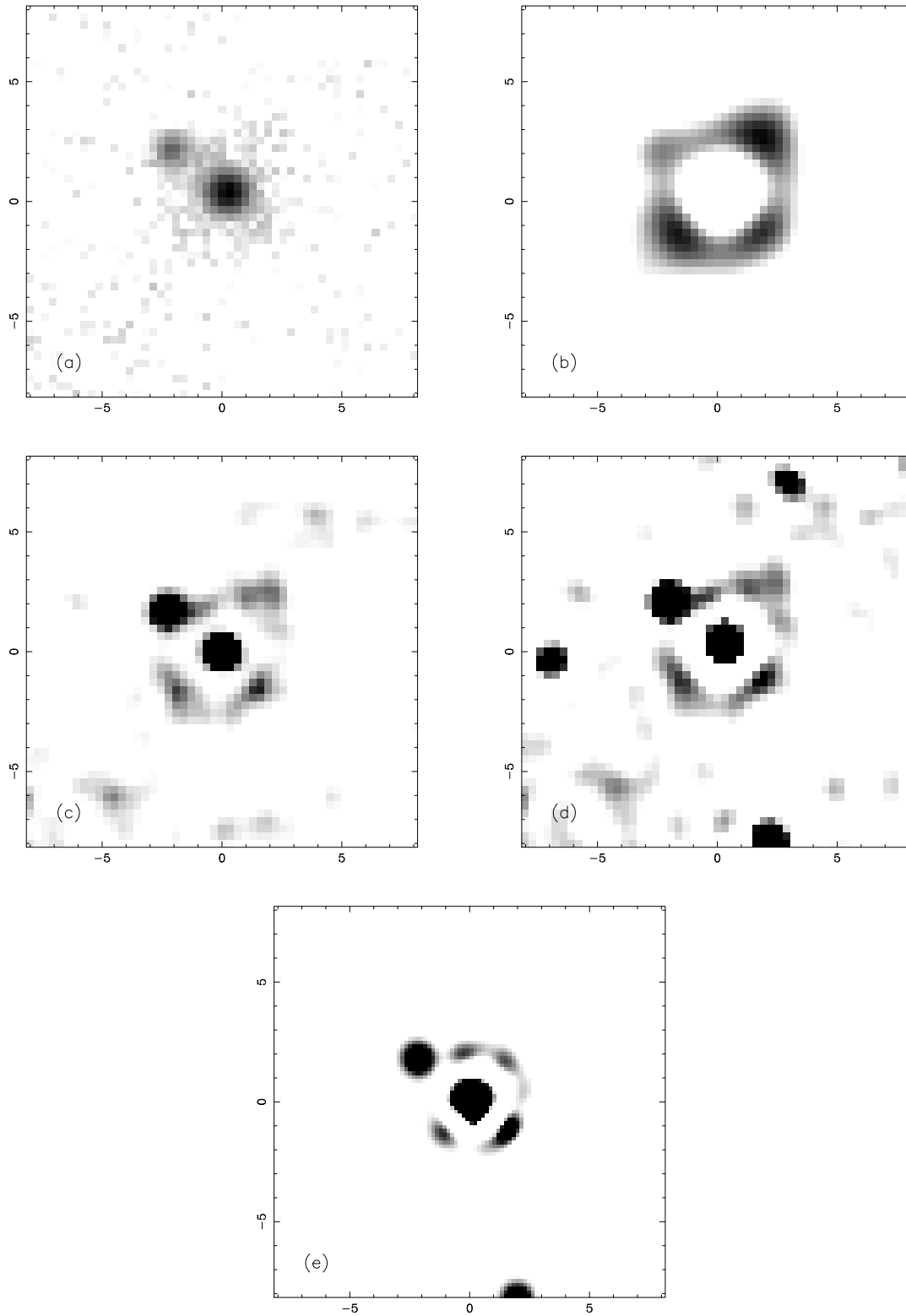


Figure 8. $H\alpha/[NII]$ images of the remnant of DY Pup. In all five plots north is up, east is to the left and the axes are marked in arcseconds. The images are: a) the original frame shown as a logarithmically grey scaled image, b) star subtracted image of the remnant (smoothed with a 2 arcsec FWHM Gaussian), c) LUCY deconvolved image, d) MEM deconvolved image, and e) CLEANED image (smoothed with a 0.64 arcsec FWHM Gaussian).

also resolves the object into a central star surrounded by a halo of extended material which more closely resembles a detached ring in this case of approximately 1.2 arcsec radius. Fig. 9(e) shows the result of the CLEAN algorithm. The results are similar to (b) and (d) although the ring does appear clumpier. This is almost certainly a result of the discrete nature of the CLEAN process and should not be regarded as a definite property of this remnant.

4 DISTANCE ESTIMATES

Given that we have obtained estimates of the angular extent of several nova shells it is possible, at least in principle, to make distance estimates based on the method of expansion parallax using measurements of the ejection velocity made during outburst. If velocities (v) are given in km s^{-1} , angular sizes (θ) in arcsec and times since ejection (t) in years then the distance (d) in parsecs is given by $d = 0.211 vt/\theta$. In all possible cases the ejection velocity is estimated from the separation of symmetric spectral features. This means that systemic velocities are not important although in any case these will be small compared with the ejection velocities.

The distance to V842 Cen has been calculated by Sekiguchi et al. (1989) using the equivalent widths of interstellar Na I D lines in their spectra. They derived a distance of $d = 0.9 \pm 0.07$ kpc. The measured diameter of the shell in our deconvolved images is about 1.6 arcsec. The time since eruption when these images were taken was 9 years. Sekiguchi et al. (1989) obtained spectra of the Balmer lines for H α to H η and saw a two peaked structure in all of the lines. The average split between the peaks was 1070 km s^{-1} . Assuming that these peaks were produced by the expanding shell we derive an expansion parallax distance of $d = 1.3 \pm 0.5$ kpc. The large errors are due to the large uncertainty in the diameter of the shell and the expansion velocity.

Marsh et al. (1983) obtained a distance estimate to BT Mon of $d = 1.8 \pm 0.3$ kpc from their long slit spectra. The expansion velocity they measure for the shell is 1800 km s^{-1} . Taking the diameter of the shell to be 10 arcsec and the time since ejection to be 56 years we also derive a distance to BT Mon of $d = 1.8 \pm 0.3$ kpc. These estimates are limited by the poor velocity resolution of Marsh and higher resolution spectra combined with our imaging data would enable a better estimate to be made.

Payne-Gaposchkin (1957) adopts a value of 1600 km s^{-1} for the velocity of the ejecta of CP Pup. If we take this value along with a shell diameter in 1995 of 19.5 arcsec then the derived distance is $d = 1.8 \pm 0.4$ kpc. The uncertainty arises from assuming the velocity of the shell is known to an accuracy of 400 km s^{-1} .

McLaughlin (1960) derives a distance to RR Pic of 480 pc from the angular expansion of the knots of the ejecta (taken from Williams and Gallagher 1979). Payne-Gaposchkin (1957) presents results for the time evolution of a variety of different lines. There are a consistent set of velocities through the decline at $\pm 400 \text{ km s}^{-1}$. Assuming the equatorial ring is in fact circular then we derive an inclination angle of $70 \pm 5^\circ$. Correcting the observed line of sight ejection velocity for this angle we get an intrinsic velocity of 850 km s^{-1} . The observed major axis of the ring was 21

arcsec so we then derive a distance to RR Pic of 600 ± 60 pc. This is slightly larger than that of McLaughlin as it also takes into account the inclination angle of the aspherical shell.

We could find no published information on expansion velocities for RR Cha, DY Pup and HS Pup and so no distance determinations were possible.

The distances derived in this section are uncertain for two obvious reasons – the uncertainties in our estimates of shell diameters and the measurements of ejection velocities obtained from the literature. However, the discussion of RR Pic also raises the important point that distance estimates based on expansion parallax in the manner we describe here generally assume spherically symmetric ejection i.e. the ejection velocity is obtained from doppler shifts along the line of sight whilst shell diameters are obtained from expansion in the plane of the sky. It is clear from these images and those presented in Slavin et al. (1995) that many nova shells are far from spherical. Thus more accurate measures of distance will require some knowledge of the geometry of the shell. This can only be derived by combining spatially-resolved spectroscopy and imaging. In papers to follow we present the results of such spectroscopy/imaging for several of the more extended shells in our northern-sky sample.

5 DISCUSSION

Of the 17 novae without previously detected shells which were imaged 4 new shells were detected. The new material discovered was not resolved from the central systems in any of these cases although scaled contour maps (see Fig. 1) and brightness profiles (see Fig. 2) clearly proved that they were extended. To investigate the morphology of these shells star subtraction, Richardson-Lucy, MEM and CLEAN deconvolutions were used. Input PSFs to the routines were stars from the same frames which had brighter peak intensities than those of the central systems of the novae to allow proper sampling of the wings of the PSFs. The results of these different methods were in general agreement allowing some confidence in the predicted shell structures. Notably, extended tails similar to those previously detected in DQ Her (Slavin et al. 1995) have been discovered in the shell of RR Pic (see also O'Brien & Slavin 1996).

Further analysis of, for example, the bipolarity of these shells is not advisable due to the limitations of ground-based imaging of such small angular-scale structures. However Hubble Space Telescope observations of several of these objects are scheduled and will hopefully improve on these data although it should be noted that the observations in this paper are relatively long exposures using a 4m-class telescope. High-resolution spectroscopy of these objects should also be obtained which, when combined with these images will enable distance estimates via expansion parallax as well as further insight into the detailed structure of the more extended objects.

6 ACKNOWLEDGEMENTS

We thank Keith Taylor and Joss Bland-Hawthorn for support at the Anglo-Australian Observatory, Brent Tully for

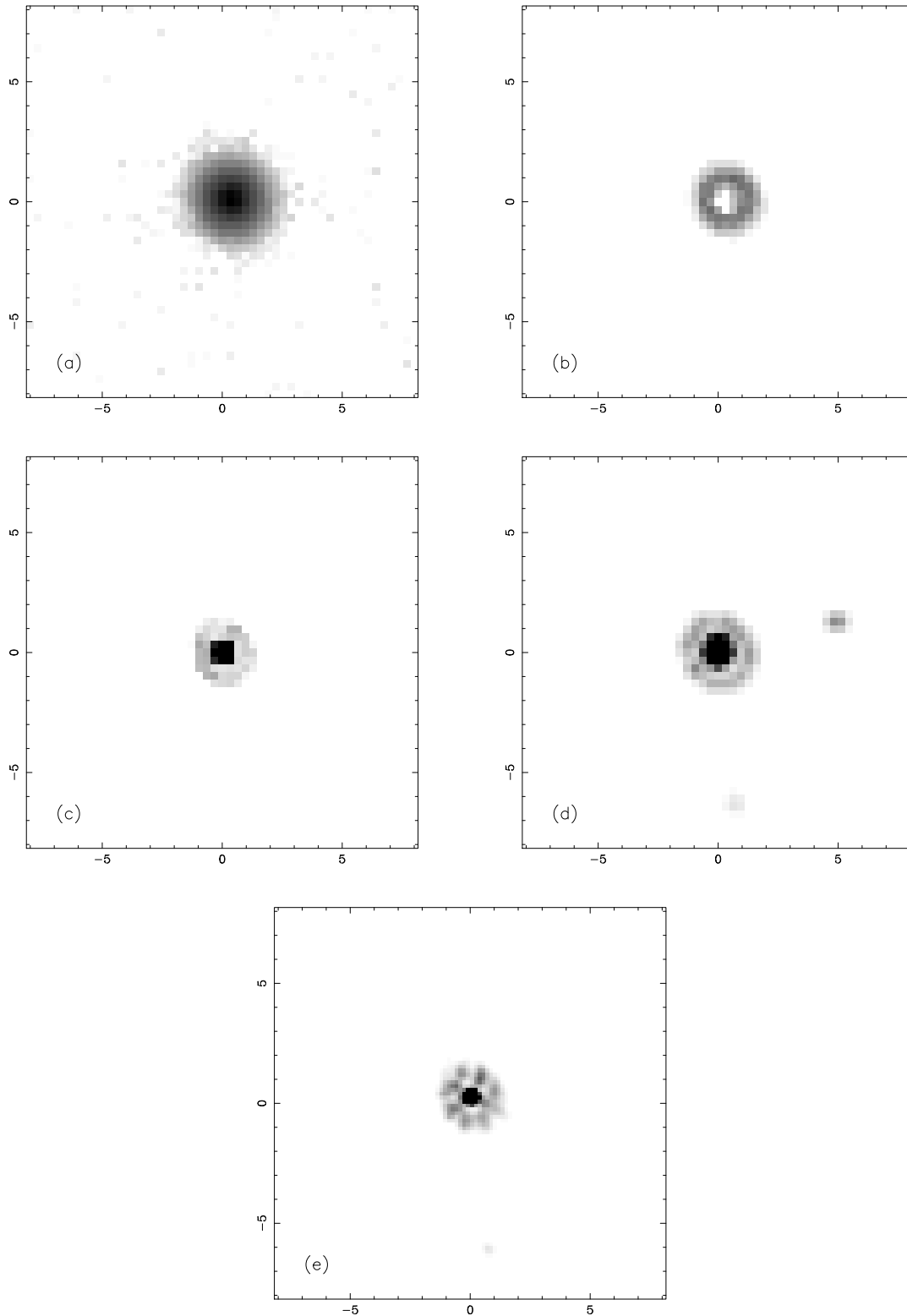


Figure 9. $H\alpha/[NII]$ images of the remnant of HS Pup. In all five plots north is up, east is to the left and the axes are marked in arcseconds. The images are: a) the original frame shown as a logarithmically grey scaled image, b) star subtracted image of the remnant, c) LUCY deconvolved image of the remnant, d) MEM deconvolved image of the remnant, and e) CLEANed image (smoothed with a 0.64 arcsec FWHM Gaussian).

the loan of filters and Andy Slavin for discussions regarding the northern-sky survey. CDG acknowledges support from a PPARC studentship.

REFERENCES

- Bode M. F., Evans A., 1989, *Classical Novae*, Wiley & Sons Ltd., Chichester
- Bowen I.S., 1956, *AJ*, 61, 336
- Duerbeck H.W., 1981, *PASP*, 93, 165
- Duerbeck H.W., 1987, *A Reference Catalogue and Atlas of Galactic Novae*, D. Reidel, Dordrecht
- Evans A., Bode M.F., Duerbeck H.W., Seitter W.C., 1992, *MNRAS*, 258, 7 (
- Marsh T.R., Oke J.B., Wade R.A., 1983, *MNRAS*, 205, 33P
- McLaughlin, D.B., 1960, in *Stellar Atmospheres*, p585, ed. J.L. Greenstein, University of Chicago Press, Chicago
- O'Brien T.J., Slavin A.J., 1996, in *Cataclysmic Variables and Related Objects*, Proc. IAU Coll. 158, p309, ed. A. Evans & J.H. Wood, Kluwer, Dordrecht
- Payne-Gaposchkin C., 1957, *The Galactic Novae*, Dover Publications Inc., New York
- Schaefer B.E., Patterson J., 1983, 268, 710
- Sekiguchi K., Feast M.W., Fairall A.P., Winkler H., 1989, *MNRAS*, 241, 311
- Slavin A.J., O'Brien T.J., Dunlop J.S., 1994, 266, L55
- Slavin A.J., O'Brien T.J., Dunlop J.S., 1995, 276, 353
- White J.C. II, Honeycutt R.K., Horne K., 1993, *ApJ*, 412, 278
- Williams R.E., Gallagher J.S., 1979, *ApJ*, 228, 482
- Williams R.E., 1982, *ApJ*, 261, 170